

Operational Analysis of Vertiport Surface Topology

Shannon Zelinski
NASA Ames Research Center
Moffet Field, CA, USA
shannon.j.zelinski@nasa.gov

Abstract - Urban Air Mobility (UAM) concepts and technologies are being developed to safely enable operations of small, electric-powered or hybrid, pilot-optional, vertical-takeoff-and-landing (VTOL) passenger and cargo aircraft at vertiport facilities in urban and suburban environments. It is likely that many of the highest demand locations for vertiports will be in space constrained urban environments, requiring vertiport designs to maximize throughput within a compact surface footprint. This paper presents several generic vertiport topology design approaches and evaluates their relative surface area utilization and operational efficiency under different wind constrained configurations while meeting safety driven spacing constraints derived from heliport design standards and subject matter expert interviews.

Keywords—urban air mobility, vertiport design, surface operations

I. INTRODUCTION

Urban Air Mobility (UAM) concepts and technologies are being developed to safely enable operations of small, electric-powered or hybrid, pilot-optional, vertical-takeoff-and-landing (VTOL) passenger and cargo aircraft at vertiport facilities in urban and suburban environments. To realize door-to-door time savings for trips as short as 20 miles, UAM concepts envision passengers flying VTOL aircraft that can be summoned “on-demand” between local vertiports close to their origin and destination [1]. In order to be economically viable for operators, service providers and the travelling public, orders-of-magnitude more aircraft and vertiports than operate today would be required [2]. Studies of potential UAM markets have shown that demand on popular destinations will require vertiports to have multiple touchdown and liftoff (TLOF) areas. A preliminary assessment of the number of TLOFs required to support a representative UAM demand network applied to Fort Worth, TX estimated a need for 98 TLOFs distributed among 25 locations during peak traffic [3]. Although this estimate averages to four TLOFs per location, 75% of the total demand was captured by seven locations suggesting that the required TLOFs could be closer to ten for some locations. In order to maximize the throughput of TLOFs, aircraft will need to taxi (or be conveyed) to parking areas for turnaround (unloading, loading, battery charging etc.) to free up TLOFs for arrival and departure operations. Initial work in vertiport design [4] characterized relationships between numbers of TLOFs and parking areas and ranges of assumed time requirements for TLOF operations, taxi, and turnaround time at parking spaces. For example, five parking spaces per TLOF achieved maximum TLOF utilization based on 60 sec arrival or departure operations, 15 sec taxi time, and 300 sec turnaround time. It is likely that many of the highest

demand locations will be in space constrained urban environments, requiring vertiport designs to maximize throughput within a compact surface footprint. This presents an interesting operational challenge for designing safe, efficient, and compact vertiport surface topologies. Vertiport designs must consider space requirements of surface features like TLOFs, parking gates, taxiways, and passenger accommodation areas. They must also consider airspace constraints which could affect arrival and departure paths to the vertiport, including surrounding tall buildings, obstructions, noise restrictions, neighboring traditional-controlled airspace, winds, zoning, etc.

There has not been much work exploring vertiport design standards. For example, one study exploring landing accuracy considerations for UAM, showed that representative models of electric VTOL aircraft for UAM can land within a radius of 20-30 ft 95% of the time under general light turbulence conditions [5]. This only scratches the surface of developing standards for vertiport TLOF space requirements. However, existing heliport design standards [6] provide an excellent starting point for exploring vertiport topology design.

This paper presents several generic vertiport topology design approaches and evaluates their relative surface area utilization and operational efficiency while meeting safety driven spacing constraints derived from heliport design standards and subject matter expert interviews. Section II describes the assumed vertiport attribute and constraints as well as three surface topology design approaches based on how taxiways are used to connect TLOFs and parking pads. Section III presents the surface area utilization analysis of the three design approaches as the number of parking spaces per TLOF increases. Section IV presents a model for mapping wind heading and speed to feasible vertiport TLOF configurations for accommodating approach and departure operations. In Section V operational efficiency is analyzed under each feasible configuration from this model. Section VI discusses the relative advantages and disadvantages of the three design approaches, and the paper is concluded in Section VII.

II. VERTIPORT TOPOLOGY DESIGNS

A. Design Attributes

This section discusses assumptions and constraints driving the design attributes for this analysis. It is assumed that the density of operations at a single vertiport will be great enough to require multiple independent TLOFs. For this analysis, each vertiport design contains four TLOFs. Because many high demand vertiport locations will be within space constrained urban environments, it is assumed that a minimum surface

footprint is desired. The most compact configuration of four TLOFs is a square. For this analysis, each vertiport design utilizes a square surface footprint with one TLOF at each corner. Placing TLOFs at the corners also maximizes the arcs of airspace available for independent approach and departure operations to/from each TLOF without constraining surface features. It is assumed that the area immediately surrounding the surface is free of airspace obstructions that would interfere with approach/departure paths to these corner TLOFs. In order to maximize the throughput of TLOFs, it is assumed that aircraft will taxi or be conveyed to parking areas for turnaround to free up TLOFs for approach and departure operations. Therefore, each vertiport design must include taxi paths from each TLOF to multiple parking spaces. Taxi paths may be placed between multiple TLOFs as well to give aircraft using a particular parking space the option of using different TLOFs depending on the operating conditions. Whether the vertiport is at ground level or raised, the surface will still require space for passengers to access the aircraft for loading and unloading. For each design approach considered, priority is given to maximizing parking spaces and accommodating the required taxi paths, with any remaining space given to passenger access. It is assumed that any centrally located passenger area may be accessible from below the vertiport surface.

B. Surface Feature Constraints

In the absence of vertiport design standards, existing heliport design standards are used to define surface feature spacing constraints as prescribed for general aviation VFR heliports in AC 150/5390-2C [6] as follows.

1) Approach/Departure Pads

There are three components of the approach/departure pad. The TLOF is the load-bearing surface on which the vehicle lands or takes off. For multiple rotor vehicles, the TLOF is recommended to have a minimum diameter of one tip-to-tip span (TTS) which is the distance between extreme edges of spinning rotors providing vertical lift. The Final Approach and Takeoff Area (FATO) surrounds the TLOF as the area over which the pilot completes the final phase approach to land or initiates takeoff. The FATO is recommended to have a minimum diameter of 1.5x the largest dimension of the vehicle. Furthermore, FATOs must be separated by at least 200 ft to conduct simultaneous operations. The FATO Safety Area (FSA) surrounds the FATO to provide an extra margin of error in case vehicles accidentally diverge from the FATO. The FSA is recommended to extend beyond the edge of a FATO for the larger of 20 ft or 1/3 TTS. The FSA can extend past the edge of raised surfaces. For this analysis, FATO edges are placed right at the edges of the total surface area, allowing FSAs to extend past the surface boundary.

2) Taxiways

This analysis assumes vehicles will ground taxi, whether under their own power or conveyed by tug or dolly, as opposed to hover taxi. For ground taxiways, a total taxi route width of 1.5x TTS is recommended. For this analysis, the taxi route width requirement is enforced only for major taxiways connecting TLOFs. Separation requirements for minor taxiways connecting parking to the major taxiways are assumed to be satisfied by parking separation requirements discussed below.

3) Parking

To conserve space used for taxiways, this analysis assumes “back-out” or “turn-around” parking, for which a minimum diameter of the helicopter’s tail rotor arc is recommended. For the purposes of this analysis, the vehicle’s largest dimension is used as the parking pad diameter. The minimum distance between the tail rotor arcs of 10 ft for “back-out” or 1/3 rotor diameter for “turn-around” parking. For “turn-around” parking a minimum clearance of 10 ft is required between the tail rotor arc and fixed objects. This analysis assumes a minimum separation of 1/3 TTS between multiple parking spaces and between parking and an FSA, and a minimum separation of 10 ft between parking and adjacent passenger accommodation areas. It is assumed that parking spaces may access eVTOL battery charging stations without impacting space and separation requirements.

Vascik and Hansman [4] include a review of seven proposed 2-6 passenger eVTOL aircraft with maximum dimensions of 45 ft, generating TLOF, FATO, and FSA diameters of 45, 68, and 88 ft, respectively. This analysis assumes an only slightly more conservative spacing by rounding up the 1.5x largest dimension parameter and TTS to 70 ft. Fig. 1 shows a diagram of surface features and separations considered. Table I lists the surface feature separation requirements assumed for this analysis.

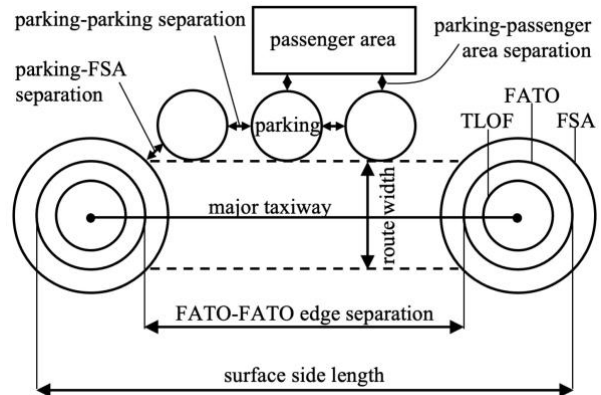


Fig. 1. Surface Features and Separations

TABLE I. SURFACE FEATURE MINIMUM SEPARATION REQUIREMENTS

Surface Feature	Requirement
TLOF diameter	45 ft
FATO diameter	70 ft
FSA diameter	100 ft
FATO-FATO edge separation	200 ft
Surface side length	340 ft
Major taxiway route width	70 ft
Parking diameter	45 ft
Parking-Parking or Parking-FSA separation	15 ft
Parking-Passenger Area separation	10 ft

C. Design Approaches

Three generic design approaches were considered based on how taxiways are used to connect TLOFs and parking pads. Surface topologies were designed for each method with up to eight parking spaces per TLOF (32 total). The minimum parking spaces per TLOF differed by design method depending on how many could fit within the minimum sized surface as defined by the FATO-FATO separation requirements for simultaneous operations. FATOs of 70 ft diameter placed at each corner of the surface separated by 200 ft requires a minimum surface side length of 340 ft.

1) Perimeter

The *Perimeter* approach places major taxiways connecting TLOFs at adjacent corners around the perimeter of the surface, with minor taxiways to parking lining the inside edge of the major taxiways. Fig. 2 shows the surface layout for the *Perimeter* design node-link model with five parking spots per TLOF (P5). Although not shown, models with different numbers of parking spaces per TLOF were also developed for analysis.

The smaller blue circles represent parking spaces. Each complete green circle represents a FATO with FSA arc surrounding it to the edge of the surface. Green lines represent major taxiways connecting green nodes at the center of each TLOF. Similarly, blue lines represent minor taxiways connecting major taxiways to blue nodes at the center of each parking space. The light green shaded region marks the 70 ft wide area required by the major taxiways. The light blue shaded region marks the area used by parking. This includes 10 ft separation from the light orange shaded region marking remaining area available for passenger accommodation.

Each *Perimeter* node-link model is developed by first placing parking nodes arranged in square shape spaced 60 ft (45 ft parking diameter + 15 ft separation) from each other. Major taxiways are then wrapped around the parking spaces. Due to the parking-FSA spacing requirements for the corner parking spots, the edge of the major taxiways is placed an extra 2 ft from the edge of the parking spaces such that the major taxiway centerline is 59.5 ft ($70/2 + 45/2 + 2$) ft from the parking nodes.

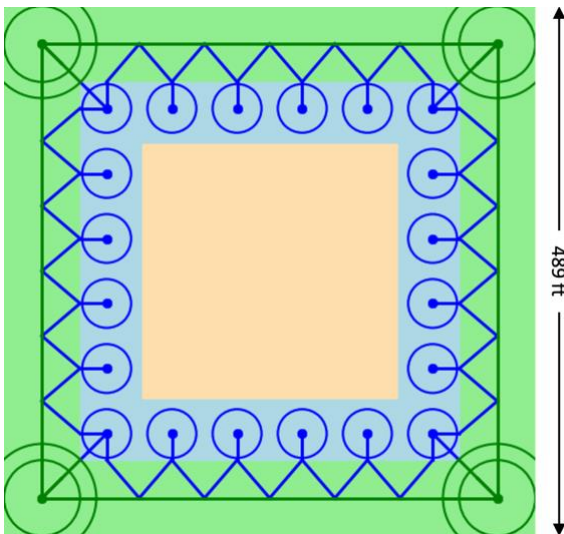


Fig. 2. *Perimeter* design with 5 parking spaces per TLOF (P5)

TLOF nodes are placed at the intersections of major taxiways. Minor taxiways head straight out from the parking node to stay clear of adjacent parking spaces until they reach the edge of major taxiway. The minor taxiways then angle toward one of the TLOF nodes at either end of the major taxiway such that they intersect the major taxiway centerline at the same point as an adjacent minor taxiway heading in the opposite direction. Only corner parking nodes have direct access to TLOF nodes without joining a major taxiway.

Perimeter node-link models were developed with as many as eight parking spaces per TLOF (P8) down to only two parking spaces per TLOF (P2) for which the minimum surface width of 309 ft is less than the 340 ft width required for independent operations. P2 was redesigned from the outside in, placing parking the same relative distance from TLOFs and major taxiways as the other *Perimeter* designs but with parking-parking spacing larger than the minimum 15 ft.

2) Central

The *Central* approach places major taxiways connecting TLOFs at opposite corners through the center of the surface, with minor taxiways to parking along the edges of the major taxiways. Figs. 3 and 4 show the surface layout for the *Central* design node-link model with five and six parking spots per TLOF (C5 and C6), respectively. Note that the surface side length for C6 is larger than for C5 to accommodate the extra parking spaces. Although not shown, additional models with different parking spaces per TLOF were also created for analysis.

Each *Central* node-link model is developed by first placing major taxiways that intersect in the center and extend out toward the corners. Parking nodes are then placed 60 ft apart along the edges of the major taxiways such that the parking space and taxiway edges touch. There is a subtle difference in the *Central* node-link design depending on whether the number of parking spaces per TLOF is odd or even. If the number of parking spaces per TLOF is odd as in Fig. 3, there will be four parking spaces closest to the middle of the surface that touch the edges of two major taxiways each close to the central intersection. If the

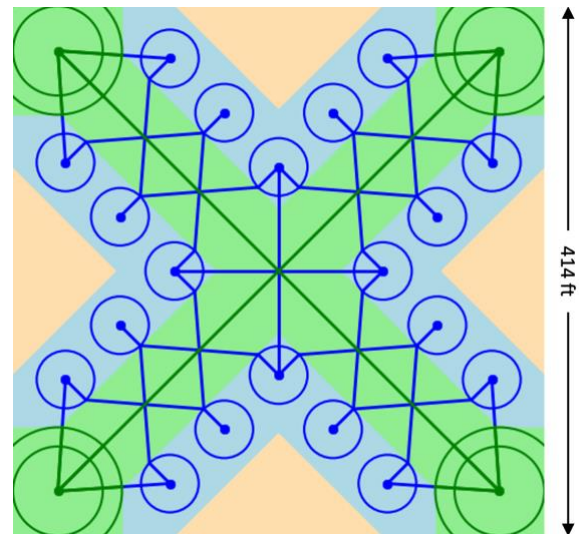


Fig. 3. *Central* design with 5 parking spaces per TLOF (C5)

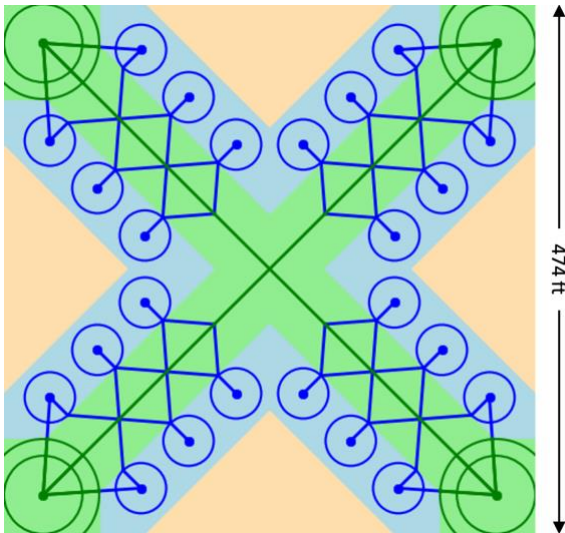


Fig. 4. Central design with 6 parking spaces per TLOF (C6)

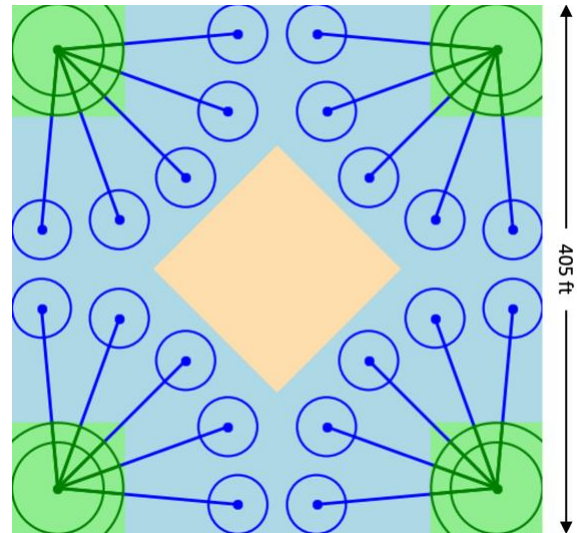


Fig. 5. Disconnected design with 5 parking spaces per TLOF (D5)

number of parking spaces per TLOF is even as in Fig. 4, each parking space will touch the edge of only one major taxiway. Once all parking nodes have been placed, the TLOF nodes are placed in the corners such that they meet parking-FSA spacing requirements (50 ft FSA radius + 22.5 ft parking radius + 15 ft separation). Minor taxiways head straight out from the parking node until they reach the edge of major taxiway, and then angle toward major taxiway intersection points equidistant from adjacent parking. The eight parking spaces closest to TLOFs are given direct access to the TLOF without joining a major taxiway. The four central parking spaces in designs with odd number of parking per TLOF, are given the option of joining the major taxiways at their central intersection as seen in Fig. 3.

Central node-link models were developed with as many as eight parking spaces per TLOF (C8) down to only three parking spaces per TLOF (C3) for which the minimum surface width of 329 ft is less than the 340 ft width required for independent operations. As with P2, C3 was redesigned from the outside in to fill out the 340 ft x 340 ft space, placing parking the same relative distance from TLOFs and major taxiways as the other Central designs but with parking-parking spacing larger than the minimum 15 ft.

3) Disconnected

The Disconnected approach uses taxiways only to connect each TLOF to multiple parking pads, not to other TLOFs. Therefore, there are no major taxiways. Fig. 5 shows the surface layout for the Disconnected design node-link model with five parking spots per TLOF (D5). Although not shown, additional models with different parking spaces per TLOF were also created for analysis.

Each Disconnected node-link model is developed by first developing one quadrant. The parking nodes were evenly spaced along an arc of fixed radius centered at the TLOF node such that parking nodes were separated by 60 ft and the two parking spaces on the edge of the arc touched the edge of the surface. Then a minor taxiway connected each parking node directly to the TLOF. This first quadrant of the design was duplicated three more times, rotated, and arranged such that the TLOFs were at

the corners of the surface and parking nodes at the edges were spaced 60 ft from those in adjacent quadrants to meet the 15 ft parking-parking spacing requirement.

Disconnected node-link models were developed with as many as eight parking spaces per TLOF (D8) down to only four parking spaces per TLOF (D4) for which the minimum surface width of 329 ft is less than the 340 ft width required for independent operations. The four quadrants of D4 were separated to reach a surface width of 340 ft so that the parking-parking spacing of the edge parking was a bit larger than the minimum 15 ft.

III. SURFACE AREA UTILIZATION ANALYSIS

Surface area utilization was analyzed by comparing the relative surface areas required for each node-link model developed. The total surface area is a square bounded by the FATO edges of the TLOF nodes placed in the corners. Total surface area is decomposed into TLOF/taxi, parking, and passenger area shown in Fig. 2-5 as light green, blue, and orange shaded regions, respectively. TLOF/taxi area includes the FSA of each TLOF node and 70 ft wide corridors along major taxi routes. Parking area includes the parking spaces as well as any additional area required to accommodate parking-parking, parking-FSA, and parking-passenger spacing requirements. Passenger area includes any large area free of taxiways that is sufficiently separated from parking. All areas are bounded by straight edges to simplify calculation.

Fig. 6 compares space utilization results for each node-link model. The same results are grouped by design approach on the top and by parking per TLOF on the bottom to facilitate comparison. As expected, the total surface area required for each design approach increases with the number of parking spaces per TLOF. The Perimeter and Central design approaches maintain fairly consistent percentages of surface area devoted to parking with a greater percentage of area shifting from TLOF/taxi to passenger as the parking per TLOF increases. Because the Disconnected design approach does not include major taxiways, its TLOF/taxi area is related to TLOF only and is fixed. As the

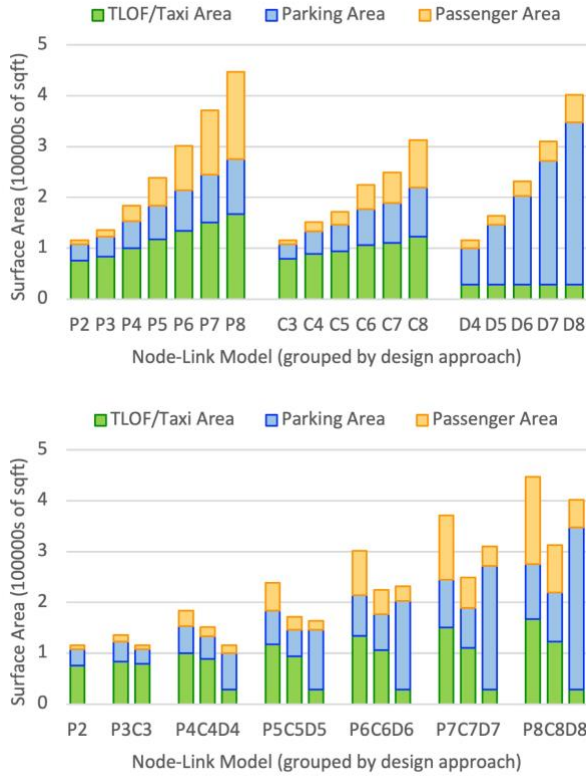


Fig. 6. Space Utilization Results

parking increases, most additional surface area is devoted to parking. This is because as the parking increases, the minor taxiways (e.g. blue lines in Fig. 5) get longer to accommodate parking-parking spacing constraints.

The smallest total surface allowable by the FATO-FATO spacing requirements (340 ft x 340 ft) accommodates two, three, and four parking spaces per TLOF for the *Perimeter*, *Central*, and *Disconnected* design approaches with respective node-links models designated as P2, C3, and D4. When comparing models with the same number of parking spaces on the bottom of Fig. 6, the *Perimeter* design approach always requires the greatest total area. However, this design also offers the greatest centralized passenger area, which may be desirable. For five or fewer parking spaces per TLOF, the *Disconnected* design approach requires the least total area. However, as parking per TLOF increases above five, *Disconnected*, requires more area than *Central*. Although *Central* appears to have a space utilization advantage over the other design at higher parking numbers, the total passenger area is actually shared among four segregated regions as seen in Figs. 3 and 4, which may be undesirable.

IV. VERTIPOINT CONFIGURATION MODEL

Vertiport operations are sensitive to wind conditions which may inhibit the use of one or more TLOFs for approach (apr), departure (dep) or both. A model is presented to map wind condition to vertiport configuration and then taxi distance and capacity metrics are presented for each configuration in the following section.

Vertiport configuration refers to the availability of individual TLOFs for approach and/or departure operations. The configuration may depend on many factors affecting arrival and departure paths to the vertiport, including surrounding tall buildings, obstructions, noise restrictions, neighboring traditional-controlled airspace, winds, zoning, and air rights. This section presents a vertiport configuration model combining static and dynamic directional constraints. Rather than limit a TLOF to a finite number of fixed approach/departure paths, it is assumed that a TLOF is available for approach and/or departure operations if there exists a large enough arch of constraint free airspace surrounding the TLOF. This approach can include any constraint expressed as radial ranges of direction relative to the TLOF. For example, if there are tall buildings or other fixed obstructions near the vertiport that would penetrate a TLOF's approach/departure surface as defined by Advisory Circular 150/5390-2C [6] to/from a certain range of directions, these ranges are included as static constraints to approach/departure operations to/from the TLOF.

For the purposes of this analysis, the only static configuration constraints considered are due to the vertiport surface. Based on heliport operations subject matter expert (SME) interviews, the approach/departure surface should not be placed over parked or taxiing aircraft or surface infrastructure like buildings or walls. To enable simultaneous operations to adjacent TLOFs, the arcs of their respective approach/departure directions should not overlap. Fig. 7 shows the resulting set of static approach/departure direction ranges to which each TLOF is constrained. The static feasible arc ranges for approaches A_s and departures D_s for an individual TLOF are equal. For example, for TLOF A, $A_s(A) = D_s(A) = [180^\circ, 270^\circ]$.

Once the static constraints are established, dynamic constraints may be incorporated that restrict the use of individual TLOFs for approach and/or departure operations under certain conditions to produce a set of possible vertiport configurations. Prevailing wind direction and speed are

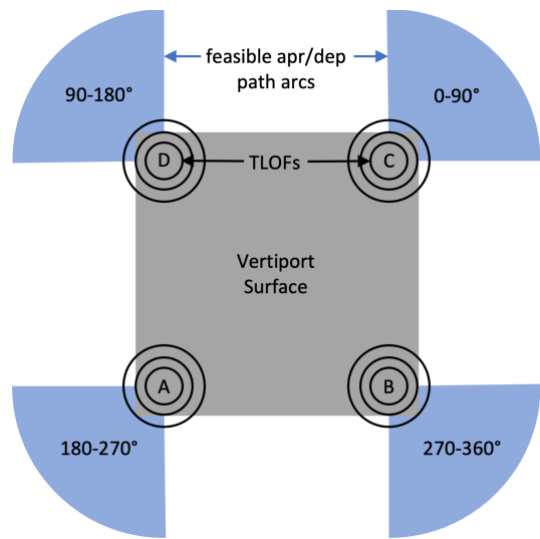


Fig. 7. Static Apr/Dep Direction Constraints

potentially highly dynamic constraint factors that were incorporated into the vertiport configuration model for this analysis. The following constraints shown in (1-2) were assumed based on heliport operations SME interviews.

$$r_w \cos(\theta_v - \theta_w) \leq 0 \text{ kt} \quad (1)$$

$$|r_w \sin(\theta_v - \theta_w)| \leq 15 \text{ kt} \quad (2)$$

where r_w , θ_w , and θ_v are the wind speed, wind direction, and vehicle direction, respectively. Equation (1) imposes the constraint that vehicles should not attempt approach or departure operations with a tailwind. A tailwind can cause the vehicle to fly into its own downwash and enter a highly unstable vortex ring state. Equation (2) imposes the constraint that vehicles should not attempt approach or departure operations with a crosswind component greater than 15 kt. Fig. 8 shows the resulting dynamic wind constraints for approach/departure direction ranges depending on wind direction θ_w and speed r_w . Unlike the static constraints, the wind feasible arc ranges for approaches A_w and departures D_w for a given wind condition are not equal. From (1) and (2), for $r_w > 0$ the wind feasible approach path arc must be within $\arcsin(15/r_w)$ of θ_w and the wind feasible departure path arc must be within $\arcsin(15/r_w)$ of $\theta_w + 180^\circ$. For example, given $\theta_w = 0^\circ$ and $r_w = 20$ kt, $\arcsin(15/20) = 49^\circ$. Therefore, $A_w(0^\circ, 20 \text{ kt}) = [0^\circ - 49^\circ, 0^\circ + 49^\circ] = [-49^\circ \text{ or } 311^\circ, 49^\circ]$ and $D_w(0^\circ, 20 \text{ kt}) = [180^\circ - 49^\circ, 180^\circ + 49^\circ] = [131^\circ, 229^\circ]$.

The combined feasible approach and departure arc ranges are the intersection of their respective static and wind feasible arc ranges given by $A(\text{TLOF}, \theta_w, r_w) = A_s \cap A_w$ and $D(\text{TLOF}, \theta_w, r_w) = D_s \cap D_w$. For TLOF A, recall from Fig.7 that $A_s(A) = D_s(A) = [180^\circ, 270^\circ]$. Therefore, $A(A, 0^\circ, 20 \text{ kt}) = [180^\circ, 270^\circ] \cap [-49^\circ \text{ or } 311^\circ, 49^\circ] = \emptyset$ and $D(A, 0^\circ, 20 \text{ kt}) = [180^\circ, 270^\circ] \cap [131^\circ, 229^\circ] = [180^\circ, 229^\circ]$. The resulting arc measurements $mA = 0^\circ$ and $mD = 229^\circ - 180^\circ = 49^\circ$ leave no feasible arc range for approaches and 49° arc range for departures. Based on heliport operations SME interviews, 15° was selected as a reasonable minimum arc measurement required to allow approach or departure operations. Therefore, in the above example, TLOF A is configured to allow departure operations but not approach operations under the given wind conditions. Fig. 9 shows the wind dependent configuration map for TLOF A assuming a 15° minimum arc measurement threshold to allow operations. When the wind conditions fall within the blue, red, or purple regions, TLOF A is configured for approach only, departure only, or dual operations, respectively. For all other wind conditions, the TLOF is closed to approach/departure operations. Fig. 10 shows the wind dependent configuration map for the entire four-TLOF vertiport with static constraints as pictured in Fig. 7. Each Apr|Dep configuration lists the TLOFs available for approach and departure operations. For example, given $\theta_w = 45^\circ$ and $r_w = 10$ kt which falls within the dark teal shaded region of the map labeled BCD|ABD, TLOFs B, C, and D may conduct approach

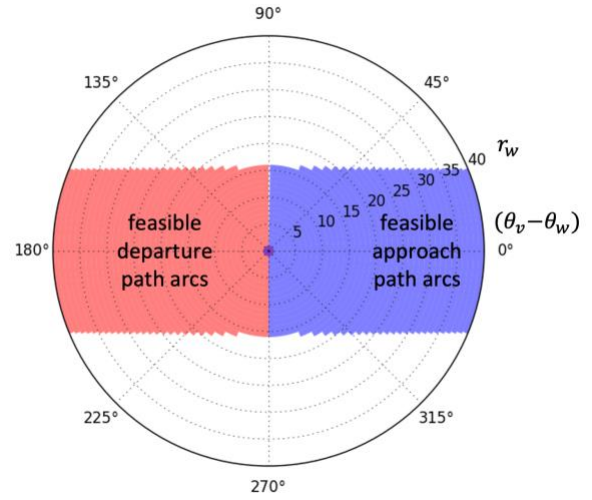


Fig. 8. Dynamic Wind Constraints for Apr/Dep Direction

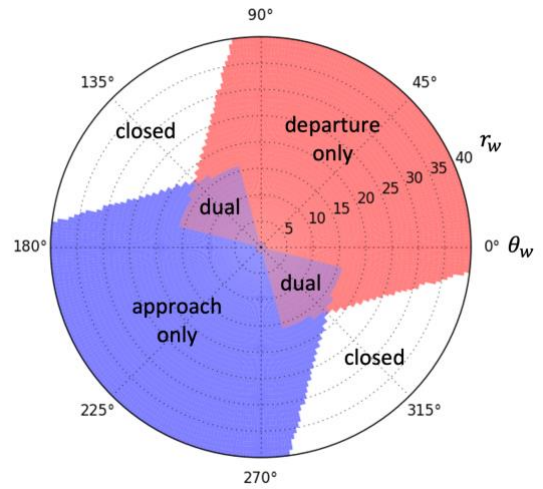


Fig. 9. TLOF A Configuration Under Different Wind Conditions

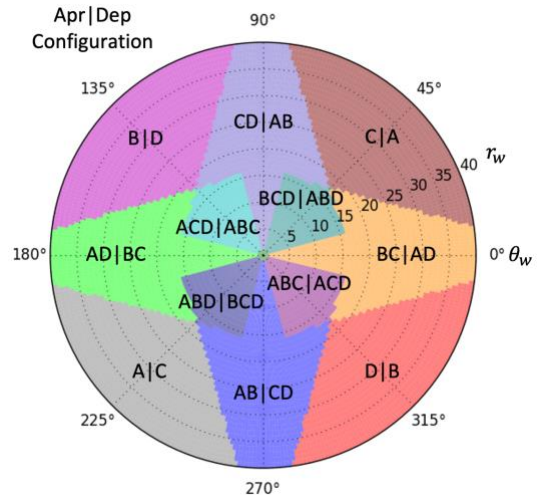


Fig. 10. Vertiport Configuration Under Different Wind Conditions

operations and TLOFs A, B, and D may conduct departure operations. The only configuration not shown in Fig. 10 due to space constraints is ABCD|ABCD which occurs only in the center of the map when $r_w = 0$ kt. The operational analysis presented in the following sections will compare results under these different vertiport configurations.

V. OPERATIONAL EFFICIENCY ANALYSIS

Due to the quadrantal symmetry of the vertiport designs analyzed, the operational efficiency results for all configurations with the same numbers of vertiports available for each operation are identical. Therefore Set 1, 2, 3, and 4 will each refer to a representative set with identical results as follows. Set 1 includes ABCD|ABCD alone. Set 2 includes ABC|ACD, ABD|BCD, ACD|ABC, and BCD|ABD. Set 3 includes AB|CD, AD|BC, BC|AD, and CD|AB. Set 4 includes A|C, B|D, C|A, and D|B.

A. Average Total Taxi Distance

This section compares average total taxi distance between each of the node-link models under each of the four different representative sets of vertiport configurations.

Routes were created between each parking space and TLOF using Dijkstra's shortest path algorithm to explore the node-link model. Parking nodes were discouraged as intermediate nodes by adding a large value cost to links that connected to parking nodes. This ensured that the resulting routes did not try to cut corners by passing through a parking node. However, TLOF nodes were allowed as intermediate nodes, which was relevant for the *Perimeter* node-link models as some TLOF-parking pairs are only reachable through other TLOF nodes. The *Disconnected* node-link models are the only ones for which routes do not exist for many TLOF-parking pairs.

Once shortest path routes were identified for each TLOF-parking pair where possible, the shortest total taxi distance using each parking spot was determined for each configuration using (3-5).

$$in_i = \min \left(\text{dist}(P_{apr}, p_i) \right) \forall P_{apr} \in \text{config} \quad (3)$$

$$out_i = \min \left(\text{dist}(p_i, P_{dep}) \right) \forall P_{dep} \in \text{config} \quad (4)$$

$$total_i = in_i + out_i \quad (5)$$

To find the shortest total taxi distance $total_i$ via parking node p_i in configuration $config$, first find the shortest taxi-in distance in_i among the routes between p_i and TLOF nodes available for approach operations P_{apr} within configuration $config$. Then, find the shortest taxi-out distance out_i among the routes between p_i and TLOF nodes available for departure operations P_{dep} within $config$. Finally, add the shortest taxi-in distance in_i to the shortest taxi-out distance out_i to get the shortest total taxi distance $total_i$. The average total taxi distance for $config$ is then the average $total_i$ for all reachable parking nodes in configuration $config$.

Fig. 11 shows the average total taxi distance results for all node-link models in each configuration set. For *Perimeter* and *Central* node-link models, all parking nodes are reachable in all configurations because there exists a route for all TLOF-parking pairs. Therefore, their results reflect total taxi distance averages across all parking nodes. However, for the *Disconnected* node-link models, the TLOF node associated with a parking node must be available for both approach and departure operations for the parking node to be reachable within a given configuration. None of Set 3 or 4 configurations have a TLOF that is available for both approach and departure operations, and so *Disconnected* node-link models have no complete taxi routes (and no total taxi distance results) in these configurations. Set 2 configurations have exactly two out of four TLOFs that are available for both approach and departure operations, and so only half of the *Disconnected* parking nodes have complete taxi routes to average total taxi distance. Only Set 1 with all four TLOFs available for both operations has complete taxi routes for all *Disconnected* parking nodes.

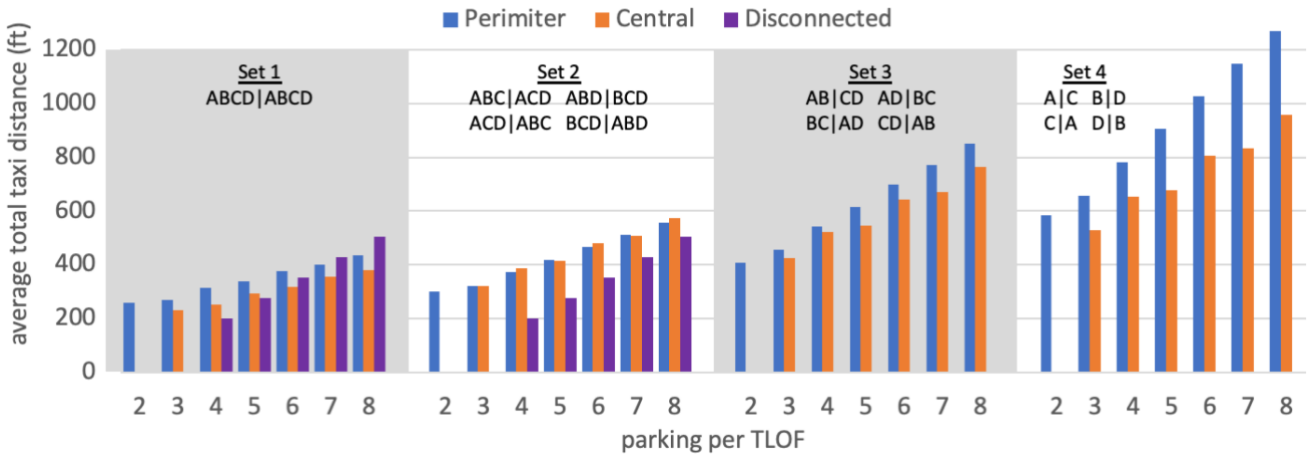


Fig. 11. Average Total Taxi Distance

Several trends can be seen in Fig. 11. For all design methods, the average total taxi distance increases with the parking per TLOF. This is because the larger surface necessitates longer taxi distances to additional parking.

The *Perimeter* and *Central* designs have increased average total taxi time for configuration sets with fewer TLOFs available for approach to departure operations. When a parking node's preferred closest TLOF is not available, it must use a longer route to get to a TLOF that is available. This effect is more pronounced for *Disconnected*. Whereas *Disconnected* designs have fewer reachable parking nodes in Set 2 than Set 1, the average total taxi distance remains constant between the two sets as these parking nodes have only one route option.

In general, the average total taxi distance is longest for *Perimeter*, followed by *Central*, and then *Disconnected*. There are some interesting exceptions of note. As the *Disconnected* total taxi distance become longer as parking is added, the average total taxi distance starts to exceed *Central* at six parking spaces per TLOF, and exceeds *Perimeter* as well for parking per TLOF greater than six. In Set 2, the *Perimeter* and *Central* average total taxi times are almost identical.

B. Operational Capacity

This section analyzes the theoretical operational capacity of each node-link model in each configuration set. Guerreiro et al. [8] introduced a theoretical model for comparing surface capacity with TLOF capacity to determine if a vertiport's capacity was limited by its parking or TLOFs. This analysis adopts a similar method shown in (6-7)

$$C_{surf} = N_{park} \cdot \frac{t_{window}}{t_{taxi} + t_{park}} \quad (6)$$

$$C_{apr/dep} = N_{TLOF} \frac{t_{window}}{t_{apr} + t_{dep}} \quad (7)$$

where C_{surf} is the number of surface operations that can be processed in time window t_{window} and $C_{apr/dep}$ is the number

of balanced TLOF operations (pair of approach/departure operations) that can be processed in t_{window} . N_{park} is the number of reachable parking nodes. Parking nodes that have no complete taxi routes to operational TLOFs are excluded from this count. N_{TLOF} is the number of operational TLOFs, regardless if they are dedicated to either approach or departure operations or if they allow both. Only TLOFs unavailable for approach or departure operations are excluded from this count. Heliport operations SME interviews identified the rule of thumb for VTOL ground taxi speed to be equivalent to "a brisk walk" (~2.7 mph or 4 ft/s) regardless of whether the vehicle taxis under its own power or is conveyed. The total taxi time t_{taxi} was calculated from the average total taxi distance results shown in Fig. 11 using an average taxi speed of 4 ft/s. The total time spent at the parking node t_{park} was selected to be a constant value of 8 min (480 sec) based on assumed separate loading and unloading times of 60 sec per passenger (used in [7-8]) and an average of 4 passengers for the 2- to 6-passenger eVTOL vehicles envisioned. Vehicle charging times in excess of these 8 min are not considered in this analysis. Therefore, it is assumed that either vehicles charge for this short period of time or return to other vertiports for more charging. The TLOF utilization time for approach t_{apr} and departure t_{dep} operations is assumed to be 60 sec each also used in [7-8]. A t_{window} of 15 minutes is arbitrarily chosen to compare capacity results. Table II shows the resulting $C_{apr/dep}$ for each vertiport design approach and configuration set.

TABLE II. APPROACH/DEPARTURE OPERATIONS CAPACITY

Design/Configuration	Set 1	Set 2	Set 3	Set 4
<i>Perimeter</i>	30	30	30	15
<i>Central</i>	30	30	30	15
<i>Disconnected</i>	30	15	0	0

Fig. 12 shows the C_{surf} results for each node-link model and configuration set. The $C_{apr/dep}$ results from Table II are also shown as black lines underlying the C_{surf} bars of relevant

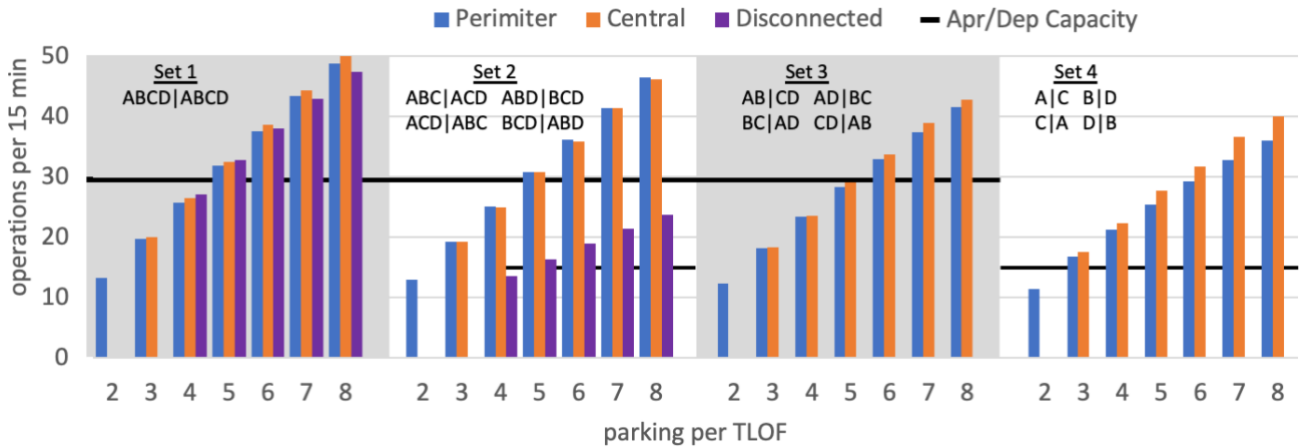


Fig. 12. Surface Operations Capacity

configuration sets for easy comparison. The surface capacity increases with parking per TLOF as additional parking availability counteracts the effect that increasing average taxi distance has in increasing average taxi time. However, this effect can be seen as surface capacity tends to decrease for configuration sets with fewer TLOFs available for approach/departure operations and therefore longer taxi distances and times. The impact of reduced number of reachable parking nodes for *Disconnected* node-link models in Set 2 in reducing surface capacity is even more dramatic. Due to slightly shorter average total taxi distances, *Central* surface capacity is slightly higher than that of *Perimeter* for all configurations but Set 2 where they are similar just like their average total taxi distances. For a parking per TLOF of five or greater, the surface capacity is either very similar to or greater than approach/departure capacity for all configurations.

VI. DISCUSSION

The operational efficiency results suggest that five parking spaces per TLOF may be sufficient given the assumed values for average taxi speed, t_{park} , t_{appr} , and t_{dep} . The designs with five parking spaces per TLOF are pictured in Figs. 2, 3 and 5.

From an operational efficiency perspective, *Disconnected* is at a clear disadvantage when TLOFs are restricted from performing both approach and departure operations for any reason. *Disconnected* may have comparable capacity to other methods under configuration Set 1. However, keep in mind that Set 1 consists of only a single configuration made possible under completely calm wind conditions. The greatest advantage of *Disconnected* is in its surface area utilization by offering the greatest number of parking spaces (four per TLOF) in the smallest allowable surface area for four independent TLOFs. At five parking spaces per TLOF, the required total surface area for *Disconnected* becomes comparable with *Central* and this advantage is lost. Although not analyzed in this paper, *Disconnected* may have an advantage with respect to surface congestion. As all its routes between TLOFs and parking are completely independent of one another, the *Disconnected* approach should not be susceptible to surface congestion which could potentially reduce the operational efficiency of *Perimeter* and *Central* designs dependent on interconnected taxiways. A possible *Disconnected* design enhancement for future analysis would be to connect parking spaces between adjacent quadrants with minor taxiways where possible. For example, as seen in Fig. 5, the pairs of parking spaces at the edges of the surface directly across from one another could be connected to allow through access to each other's TLOF. This could provide some capacity improvement in configurations where TLOFs are restricted to only one type of operation.

Even though *Central* tends to have shorter average total taxi distance, it is on fairly equal footing with *Perimeter* when it comes to capacity, and both are robust to configuration adjustment to wind condition. The primary advantage of *Central* over *Perimeter* is that it requires less total surface area for the same amount of parking. A possible disadvantage is that whereas *Perimeter* passenger area is centralized, the *Central* passenger area is segregated into four separate areas which may present different passenger access and accommodation considerations.

This analysis focused on four-TLOF square-shaped vertiport designs. It would be interesting to extend this analysis to rectangular designs and designs incorporating more than four TLOFs to determine if any more capacity can be gained and what the impact would be to surface area requirements. As this paper presented a purely analytical evaluation of theoretical capacity limits, it would be interesting to see what efficiency is lost in simulation where surface congestion may become an issue.

VII. CONCLUSION

This paper presented three generic methods for vertiport surface topology design based on how taxiways are used to connect TLOFs and parking. Analyses of surface area utilization and operational efficiency produced some interesting insights into the advantages and disadvantages of the different design approaches. The *Disconnected* approach focuses on maximizing parking per TLOF without providing taxi connectivity between multiple TLOFs. Whereas this approach does provide the greatest amount of parking in the smallest total surface area, it is not robust to conditions where TLOFs may be restricted from performing both approach and departure operations for any reason. The *Perimeter* and *Central* design methods provide connectivity between multiple TLOFs by placing major taxiways around the perimeter and through the center of the vertiport surface, respectively. These approaches are both robust to configuration adjustments due to wind conditions. Whereas the *Central* approach requires less surface area, *Perimeter* provides a centralized passenger area rather than segregating into four areas like *Central*. The operational capacity analysis suggests that five parking spaces per TLOF may be sufficient assuming 60 sec TLOF utilization time for approach and departure operations, 4 ft/s taxi speed, and 8 min turnaround time at parking spaces. If longer turnaround times are desired for charging purposes, more parking may be desired.

This paper also introduced a method of combining static and dynamic approach/departure directional constraints into a vertiport configuration model. This model may be used to analyze other vertiport surface design robustness to configuration change or integrated into fast-time simulations of vertiport surface operations. It can also be utilized to look into the design of vertiports placed on large airports with traditional traffic arrival and departure paths added as constraints.

ACKNOWLEDGMENT

The author thanks Rex Alexander for invaluable support as a heliport operations subject matter expert.

REFERENCES

- [1] J. Holden and N. Goel, "Fast-forwarding to a future of on-demand urban air transportation," UBER Elevate white paper, October 27, 2016. www.uber.com/us/en/elevate/
- [2] E. Mueller, P. Kopardekar, and K. Goodrich, "Enabling airspace integration for high-density on-demand mobility operations," 17th AIAA Aviation Technology, Integration, and Operations Conference, 5-9 June 2017, Denver, Colorado.

- [3] K. H. Goodrich and B. E. Barmore, "Exploratory analysis of the airspace throughput and sensitivities of an urban air mobility system," 18th AIAA Aviation Technology, Integration, and Operations Conference, 25-29 June 2018, Atlanta, Georgia.
- [4] P. D. Vascik and R. J. Hansman, "Development of vertiport capacity envelopes and analysis of their sensitivity to topological and operational factors," AIAA SciTech Forum, 7-11 January, 2019, San Diego, California.
- [5] E. Yilmaz, M. M. Warren, and B. J. German, "Energy and landing accuracy considerations for urban air mobility vertiport approach surfaces," AIAA Aviation Forum, 17-21 June 2019, Dallas, TX.
- [6] Federal Aviation Administration, "AC 150/5390-2C: Heliport design," 2012.
- [7] N. M. Gurreiro, R. W. Butler, J. M. Maddalon, and G. E. Hagen, "Mission planner algorithm for urban air mobility – initial performance characterization," AIAA Aviation Forum, 17-21 June 2019, Dallas, TX.
- [8] N. M. Gurreiro, R. W. Butler, J. M. Maddalon, and G. E. Hagen, "Capacity and throughput of urban air mobility vertiports with a first-come, first-served vertiport scheduling algorithm," AIAA Aviation Forum, June 2020.